Laser confocal microscopic study of pH profiles of synthetic absorbable fibers upon *in vitro* hydrolytic degradation

M. A. SLIVKA*, C. C. CHU†, Y. L. ZHANG§
Fiber Science Program, Department of Textiles and Apparel, and Biomedical Engineering Program, Cornell University, Ithaca, New York, 14853-4401, USA

The objective of this study was to develop a new and non-destructive technique to measure the interior pH of synthetic absorbable biomaterials. Such a measurement would provide the required experimental evidence for validating the postulated theory that the accumulation of acidic hydrolytic degradation products within the interior of aliphatic polyesters is responsible for the observed accelerated degradation of this class of absorbable biomaterials. This new technique used a laser scanning confocal microscope coupled with pH sensitive fluorescent dyes like Texas Red sulfonyl chloride. The capability of optical thin sectioning of a laser confocal microscope would permit a non-destructive examination of the interior of biomaterials. Poly-p-dioxanone suture fibers (PDSII) of size 2/0 were used as the model compound for this new technique. The pH values of the unhydrolyzed and partially hydrolyzed PDSII fibers were found to decrease with increasing depth from the fiber surface and reached as low as about 3.5 at 70 μm depth. The largest depth that an interior pH could be measured within absorbable biomaterials was determined by the opacity of the biomaterials, i.e. a higher depth for a less opaque material. The observed interior pH profiles were correlated to the unique morphologic structure of PDSII fibers.

1. Introduction

Research involving synthetic, biodegradable implants for a variety of applications has received great attention in recent years. Biodegradable implants obviate the need for a second surgical procedure for removal, and their gradual degradation over time minimizes long-term disadvantageous response from the body, such as stress shielding (in the case of metallic implants) and immune response. They also present a potentially ideal vehicle for the controlled release of bioactive agents, such as growth factors and antibiotics.

The majority of research activities on synthetic, biodegradable implants have centered on the use of poly(α-hydroxy acids), such as polyglycolide (PGA), poly-L-lactide (PLLA) and polydioxanone. A potential concern for using these materials has been presented based on the acidic degradation products released in the body. Both *in vitro* toxicity and *in vivo* non-specific foreign-body reactions, such as sterile sinus formation, have been reported in studies using orthopaedic implants made from PGA and/or PLLA [1–7]. Several investigators indicated that the glycolic or lactic acid-rich degradation products could significantly lower the local pH in closed and less body fluid-buffered regions surrounded by bone [8–12] or in *in vitro* degradation media [2, 13]. This is particularly true if there is a large amount of material present (such as with solid pins and rods), and if the degradation process proceeds with a burst mode (i.e. a sudden and rapid release of degradation products). This acidity may cause abnormal bone resorption and/or demineralization. The resulting environment may be cytotoxic [1, 2]. Indeed, inflammatory foreign-body reactions with a discharging sinus and osteolytic foci visible on X-ray have been encountered in clinical studies [3]. Hollinger *et al*. recently confirmed the problem associated with PGA and/or PLLA orthopaedic implants [4]. They found that a rapid degradation of a 50 : 50 ratio of glycolide-lactide copolymer in bone chambers of rabbit tibias inhibited bone regeneration. However, they emphasized that the extrapolation of *in vitro* toxicity to *in vivo* biocompatibility must consider microcirculatory capacity.

The increase in local acidity due to accumulation of acidic degradation products is also believed to accelerate hydrolysis through acid autocatalysis in the immediate vicinity of the biodegradable device. Although the higher local acidity in the interior of biodegradable implants has been proposed to explain both *in vitro* and *in vivo* data,

*Current address: OsteoBiologics Inc., University Business Park, 12500 Network, Suite 112, San Antonio, TX, 78249-3308, USA.
†To whom all correspondence should be addressed.
§Current address: Johnson & Johnson Corporate Biomaterials Center, Rm. T401, RT. 22 West, P.O. Box 151, Somerville, NJ. 08876-0151.

there are no experimental data to directly support this speculation. Such experimental evidence is difficult to obtain without a technique to directly measure the pH of the local environment.

This paper reports a new characterization method which permits scientists to measure the pH profile of the interior of absorbable biomaterials as a function of their hydrolytic degradation. This new characterization method is based upon the capability of ''optical'' thin-sectioning of a solid material by a laser confocal microscope (LCM) that was originally developed for examining the interior of biological and electronic circuit board materials. For example, Hanthamrongwit *et al*. used LCM to assess the cell morphology and distribution of keratinocytes within TissuVlies® collagen sponges [14]. Slivka and Chu have very recently extended the LCM technology from its biological domain to the study of biodegradation phenomena of absorbable composite biomaterials [15]. They reported that LCM coupled with non-reactive fluorescent dyes provides a very useful new characterization technique to examine the morphological properties of the fiber-matrix interface of totally resorbable fiber-reinforced composites upon *in vitro* hydrolytic degradation. In this paper, the interior pH profile of partially hydrolyzed 2/0 size PDSII fibers was measured as a function of depth and hydrolysis time by LCM.

2. Materials and methods

2.1. Absorbable biomaterials and *in vitro* hydrolysis

PDS-II monofilament, absorbable sutures (size 2-0 with 260 μm diameter) from Ethicon were used as the model compound for developing this new pH characterization technique. PDS-II is made from poly-p-dioxanone via ring-opening polymerization. PDS-II was chosen for this study because it is an absorbable monofilament fiber with well-characterized, reproducible, reliable and predictable properties. These suture fibers were provided in sterile, sealed packages and were subjected to *in vitro* degradation in a potassium phosphate buffered solution of 0.1 M, pH 7.44 for pre-determined periods (0, 15, 34, 43, 52, and 64 days) at 37 °C. The buffer was refreshed once every week.

2.2. Fluorescent dyes

Two fluorescent dyes were used for the measurement of the pH profile of the interior of absorbable fibers based on a fluorescence ratio imaging technique. The technique involves using a pH sensitive dye to measure the pH, together with a pH insensitive dye to factor out the effect of dye concentration on fluorescent intensity. The pH sensitive dye selected was CL-NERF (excitation 488 nm, emission 525 mm) and the pH insensitive dye selected was Texas Red sulfonyl chloride (TXR) (excitation 568 nm, emission 585 nm). Both were obtained from Molecular Probes. The pKa for CL-NERF was about 4.5, limiting its range of pH measurement to between about 3.5 and 6. Based on published findings, this range was considered acceptable for measuring local acidity. For example, Chu reported that the aqueous degradation media of polyglycolide and poly(glycolide-co-lactide) sutures decreased to a pH of 3.21–3.48 and 3.12–3.17, respectively, at the end of 70 days of *in vitro* hydrolysis [13].

Measurement of internal pH profile by LCM

LCM measurement was done using a Biorad MRC 600 interfaced with a Zeiss Axiovert 10 inverted microscope. Each of the fluorescent dyes were excited using a krypton-argon ion laser and fluorescent emission detected simultaneously using appropriate filters. Fluorescent intensity was imaged on a color scale. Using COMOS™ software, the images from each of the dyes were rasterized and ratioed, producing a new image representing the pH measurement with the concentration factored out. Images of pH below the measurable range appeared black and those above the range appeared white. The pixel values of the new image were then measured and correlated with a calibration curve, as described below.

Before a quantitative analysis of the LCM images of the PDS-II fibers could be done, a calibration curve was required to correlate the LCM measured fluorescence ratio of the two dyes to known pH values. To construct this calibration curve, aqueous solutions with known pH varying from 3 to 6.5 in increments of 0.5 were first prepared. Second, appropriate amounts of the fluorescent dye solution were added into the above-prepared solutions to make the final dye concentration within the aqueous solution equivalent to the concentration used to soak the PDS-II fiber samples. Third, the calibration solutions of varying pHs were injected into chambers made from microscope slides and cover slips (Fig. 1) and their LCM images were recorded and ratioed. The average pixel values from the ratioed images were then plot against their corresponding known pH values and a linear least-squares regression was used to construct a best line fit. The internal pH value from the testing sample could then be obtained from this best fit linear calibration equation.

After successive periods of *in vitro* hydrolysis in phosphate buffer solution at 37 °C, the PDS-II fiber samples were removed, and immediately immersed in a fluorescent dye solution consisting of a 200 mM equimolar concentration of TXR and CL-NERF in deionized water for 24 h. The samples were then removed and immediately mounted for examining the internal pH profiles. The samples were not allowed to dry throughout the analysis. All PDS-II fiber samples were mounted between a microscope slide and a cover slip for LCM imaging. The samples were immersed in the fluorescent dye solution during LCM imaging to prevent them from drying out. During analysis, the gains on the photomultiplier tubes were maintained constant after the calibration curve had been established. If it was necessary to adjust the fluorescent intensity seen by the analyzer to prevent saturation or weak reception, either the neutral density filter or the apertures were adjusted. LCM images of the PDSII fiber samples were obtained on their surface, and at regular depths toward the interior of the sample through optical thin sections. Fig. 2 illustrates the optical thin sectioning and the orientation

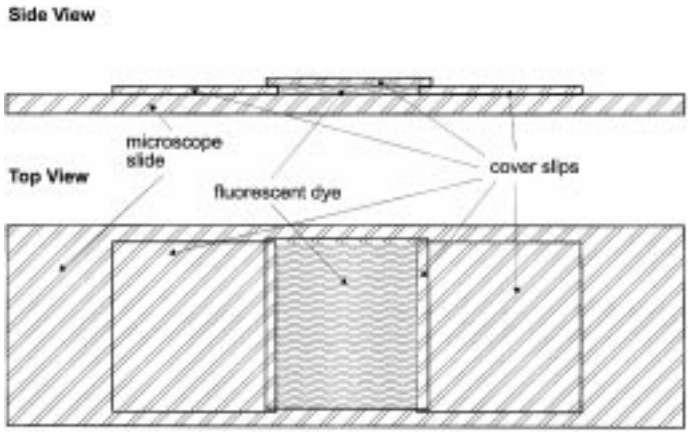

Figure 1 Schematic illustration of the set-up for establishing a calibration curve for pH measurement.

used for LCM imaging. The maximum depth that could be imaged by the present LCM system was about 70 μm beneath the surface of the PDS-II fibers, which is about 54% of the radius of the fiber. Each image of the PDS-II fiber sample was ratioed as in the construction of the calibration curve. The intensity profile was then measured along x (see Fig. 2) for the entire width of the fiber. The pH was calculated from the intensity values using the calibration curve and the profile was plotted.

3. Results

Fig. 3 shows the calibration curve constructed for all of the PDS-II samples analysis done in this study. The high R^2 value (0.98) for the linear regression supports the use of this linear calibration to calculate pH. The open circles in Fig. 3 represent pH values that are out of range for the pH sensitive dye used and thus were not used in the construction of the calibration curve. The pH of the dye solution used to soak the samples was measured using a pH meter to be about 5.6.

The internal pH profiles of the PDS-II samples from two hydrolysis times (control and 34 days) are shown in Figs 4 and 5, respectively. The data suggest that lower pH values were found at either different depth (y) or distance (x) of the fiber. The ΔpH, the magnitude of pH reduction at a particularly x and y relative to the pH on the PDSII fiber surface (i.e. $y = 0$), was the most pronounced in the middle of the fiber $(x = 0)$, but the ΔpH at a larger x location was significantly smaller than the value in the middle of the fiber. In other words, the internal pH profiles exhibited a U-shaped pattern as a function of x distance. For example, as high as $\Delta pH = 2$ at 0 μm x location was observed from the surface to 70 μm depth of the 34 days hydrolyzed PDS-II fiber, while the ΔpH at the 200 μm x location of the same fiber was only about 0.5. The possible cause for the U-shaped pattern was due to more fluid between the cover slip and the fiber at $x = 200$ μm fiber position than at $x = 0$ μm.

The ΔpH also depended on the duration of hydrolytic degradation. Initially, it increased with an increase in the duration of hydrolytic degradation, reached a maximum ΔpH value between 34 and 43 days of hydrolysis and decreased thereafter. The unhydrolyzed PDS-II fiber control (Fig. 4) also showed the same depth dependence of pH as the partially hydrolyzed fibers. At the surface of the fiber (zero depth), the pH was about 5.0–5.5, which agreed with the measured pH of the fluorescent dye solution, 5.6.

The continuous decline of pH with an increase in depth from the surface of PDS-II fibers at different periods of hydrolysis is illustrated in Fig. 6. It appears that most of the reduction in pH at any hydrolysis period occurred between 15 and 50 μm depth from the surface of PDS-II

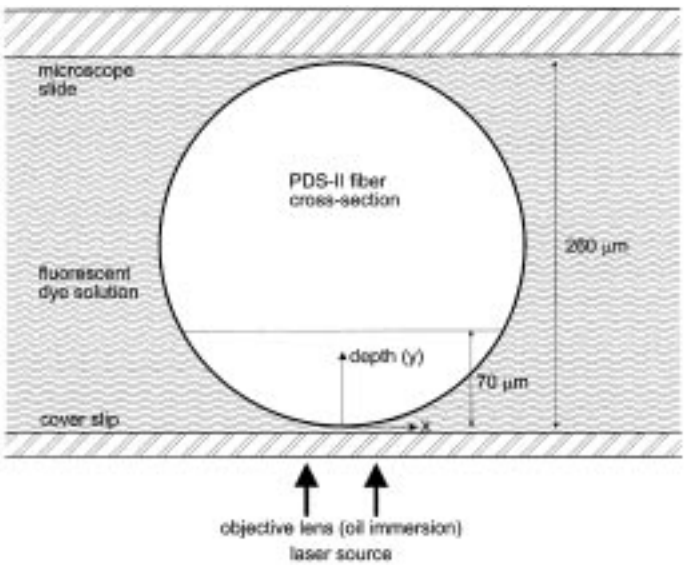

Figure 2 Schematic illustration of the orientation of the PDS-II fiber during imaging on the LCM.

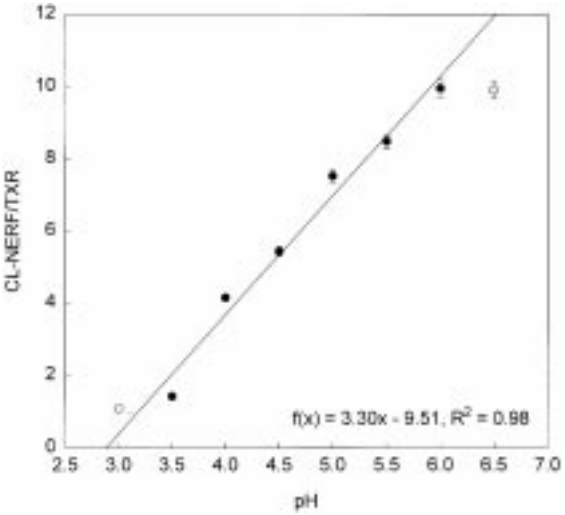

Figure 3 A calibration curve to be used for determining subsequent internal pH profiles of PDSII fibers.

fibers and was the most profound at 43 days of hydrolysis.

The 24 h fluorescent dye treatment of PDSII fibers, as required for this new characterization technique, did not result in any adverse effect on either tensile properties or surface morphology over the entire periods of hydrolysis when compared with the untreated PDSII fibers. For example, the tensile breaking force of both fluorescence dye treated and untreated 2/0 size PDSII suture fibers had 4.18 ± 0.07 and 4.24 ± 0.06 kg at 15 days, respectively, and 1.95 ± 0.01 and 2.02 ± 0.01 kg at 43 days, respectively. As shown in Fig. 7, there was no visible difference in surface morphology between the fluorescent dye treated and untreated PDS-II fibers.

4. Discussion

The ability to measure interior pH of biomaterials is essential for understanding the biodegradation mechanism and structure–property relationship of absorbable biomaterials. Such a task has not previously been accomplished without physically sectioning the samples. The availability of LCM makes such a task possible because of its unique optical thin sectioning capability.

The data presented in this paper experimentally demonstrate the generally speculated belief that solid absorbable biomaterials exhibit heterogeneous hydrolytic degradation and the core portion of the absorbable biomaterial could degrade at a faster rate than the surface layer due to the accumulated acidic degradation products in the core and subsequent autocatalysis. The level of this acid catalyzed effect, of course, depends on the size or thickness of the solid absorbable biomaterials, the level of crystallinity and orientation, and their chemical constituents. Vert *et al*. observed large voids in the interior of linear aliphatic absorbable polymers upon hydrolytic degradation and suggested that an excessive accumulation of the acidic degradation products within the polymers was the major cause for their observation of large voids [16]. Very recently, Gogolewski *et al*. showed the presence of large void space in the core of poly(D,L-lactide) and a mixture of L- and D,L-polylactide cylindrical rods (1.38 mm radius which was slightly larger than the radius of PDS-II fiber used in our study) upon *in vitro* and *in vivo* aging from 1 to 6 months [17]. At the end of 6 months *in vitro*, a very large void space about one-half of the total cross-sectional area appeared at the core of the rods. The *in vitro* aging appeared to lead to a far larger void space than the *in vivo* mode [17]. Similar findings of the appearance of large void space within the interior of absorbable biomaterials were also reported by Loh *et al*. in their study of the effect of

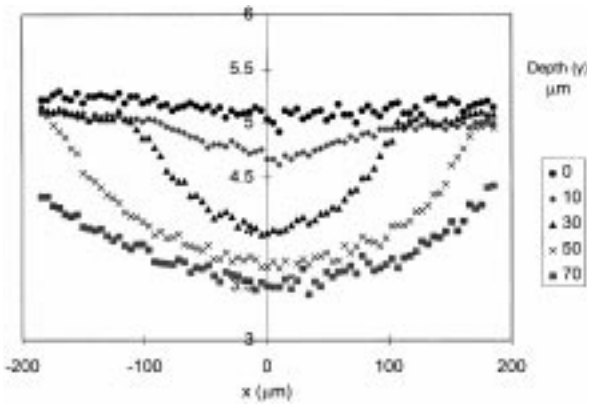

Figure 4 Internal pH profiles of unhydrolyzed 2/0 size PDSII suture fiber control as a function of both the depth and length of the fiber.

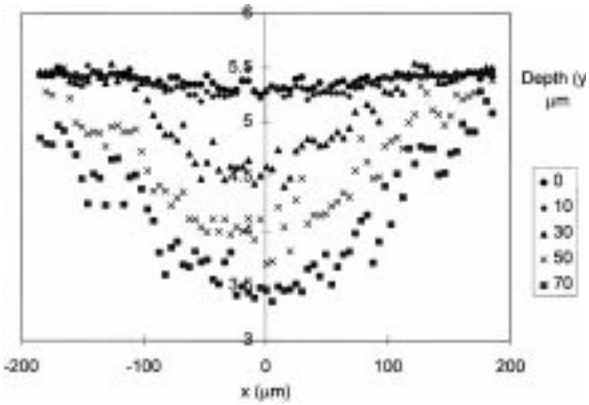

Figure 5 Internal pH profiles of 34 days hydrolyzed 2/0 size PDSII suture fiber control as a function of both the depth and length of the fiber.

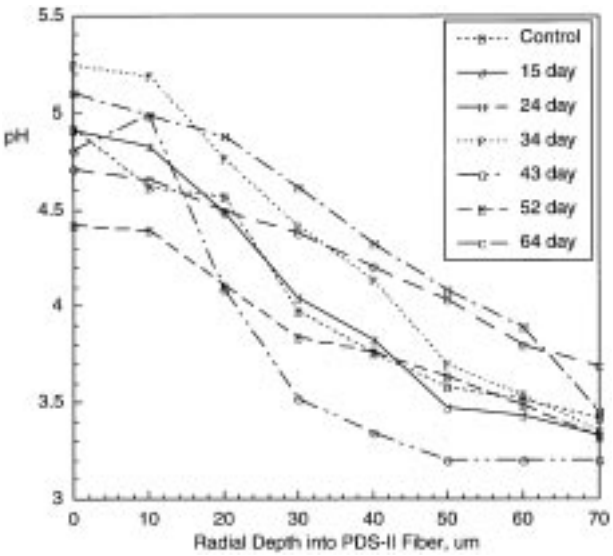

Figure 6 The change of internal pH values with the depth of 2/0 size PDSII suture fibers that were partially hydrolyzed up to 64 days.

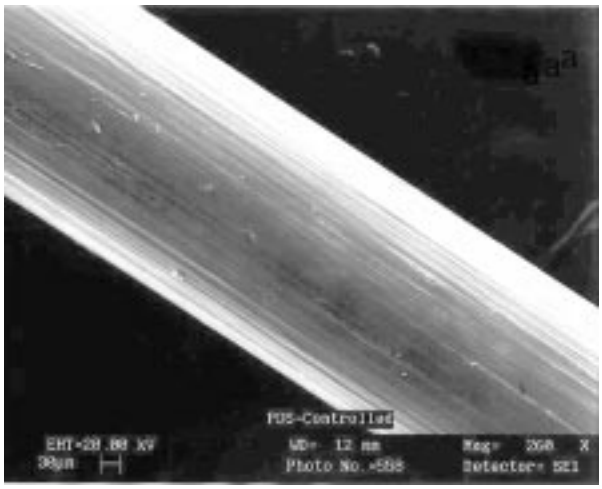

(a)

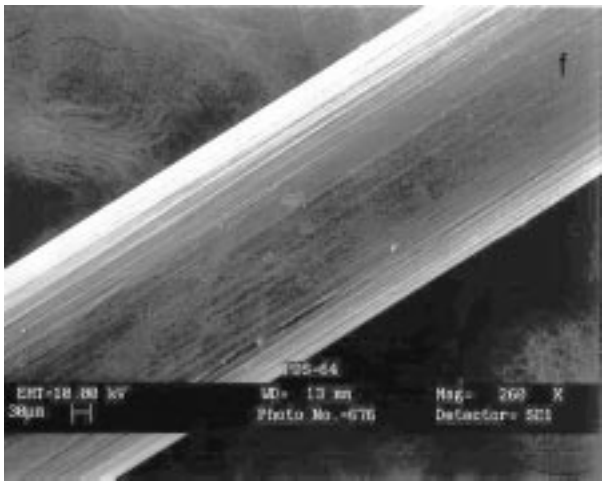

(b)

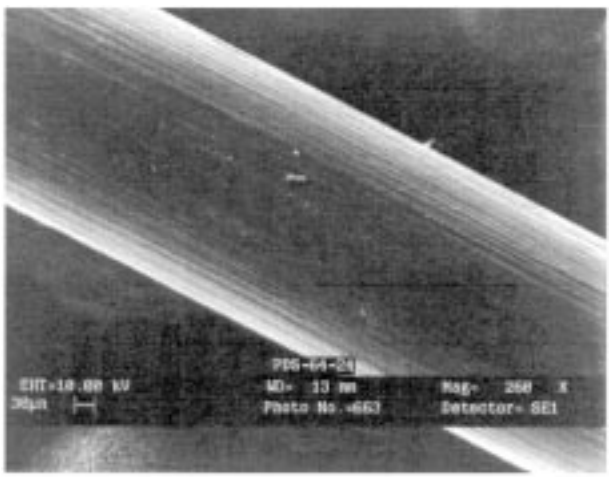

(c)

Figure 7 Scanning electron micrographs of the longitudinal view of PDSII fibers upon hydrolysis and fluorescent dye treatment. (a) unhydrolyzed PDSII; (b)64 days hydrolyzed PDSII; (c) 64 days hydrolyzed and 24 h fluorescent dye treated PDSII fiber.

plasma surface treatment on the degradation of Maxon sutures [18]. They suggested that the hydrophobic plasma surface treatment served as a barrier to reduce the accessibility of acidic degradation products from diffusing out of the core of the suture fiber and hence resulted in a faster accumulation of acids within the core that led to the observed void formation within the core of the fiber.

The interior pH profiles of the control sample were unexpected. The observed lower pH value inside an unhydrolyzed PDS-II fiber relative to its surface suggests that the fiber may have low molecular weight oligomers and residual unreacted monomer trapped within. These oligomers and residual monomers could come from either incomplete ring-opening polymerization of PDS or/and fiber melt-spinning process. A closer examination of the pH profiles as a function of depth of this control PDS-II suture fiber also revealed that there were two distinctive groups of pH profiles depending on depth, the group with depth of less than or equal to 20 µm depth and the 2nd group with 30–70 µm depth. It is possible that the inhomogeneous morphological structure of the PDS-II suture fiber is responsible for such an observation. Unlike the previously introduced PDS suture fibers, PDS-II sutures are made by subjecting the melt-spun PDS fibers to a short period of annealing at a temperature above T_m of PDS (about 125 °C) [19]. This additional heated drawing treatment, not used in PDS suture, would partially melt the surface layer of PDS fibers and subsequently modify the near-surface crystalline structure of PDS monofilament suture. Thus, a distinctive skin-core morphology that PDS sutures do not have is observed in PDS-II sutures, as shown in Fig. 8. The core of PDS-II suture has a more highly ordered and larger spherulitic crystal structure than the surrounding annular area characterized by smaller crystals.

One unexpected outcome of this study was the lack of a more pronounced correlation between the interior pH profile and degradation time of the PDS-II fiber, as demonstrated in Fig. 6. One possible reason for this is the relatively short degradation times used in this study. Although there is a lack of published biodegradation data of PDS-II, there are many published biodegradation properties of PDS suture fibers. Chu *et al*. reported that there was less than 2–3% mass loss of PDS fibers at the end of 60 days *in vitro* [20, 21] and a complete absorption was not evident until 180 days postimplantation [22–25]. Metz *et al*. reported that there was a minimal reduction in tensile breaking force of PDS fiber over a period of 35 days *in vitro* and *in vivo* [26]. Because of the slow degradation of PDS over a long period, the acidic degradation products generated inside the PDS would have ample time to diffuse out, i.e. to lessen the interior pH reduction with time. We suggest the use of faster degrading biomaterials or γ-irradiated PDS-II fibers in future studies to circumvent the requirement of a longer period of degradation for observing a more pronounced correlation between the change of interior pH profile with degradation time. Chu *et al*. had demonstrated that γ-irradiated absorbable fibers like PDS would show significantly accelerated degradation [20]. This could lead to a significant accumulation of acidic degradation products within a short period, i.e. a more profound change in the interior pH profile with degradation time.

As with any new technique, there are some limits of using LCM to examine the internal pH profiles of absorbable biomaterials. One major limit of this reported new technique will be the depth of the biomaterial that

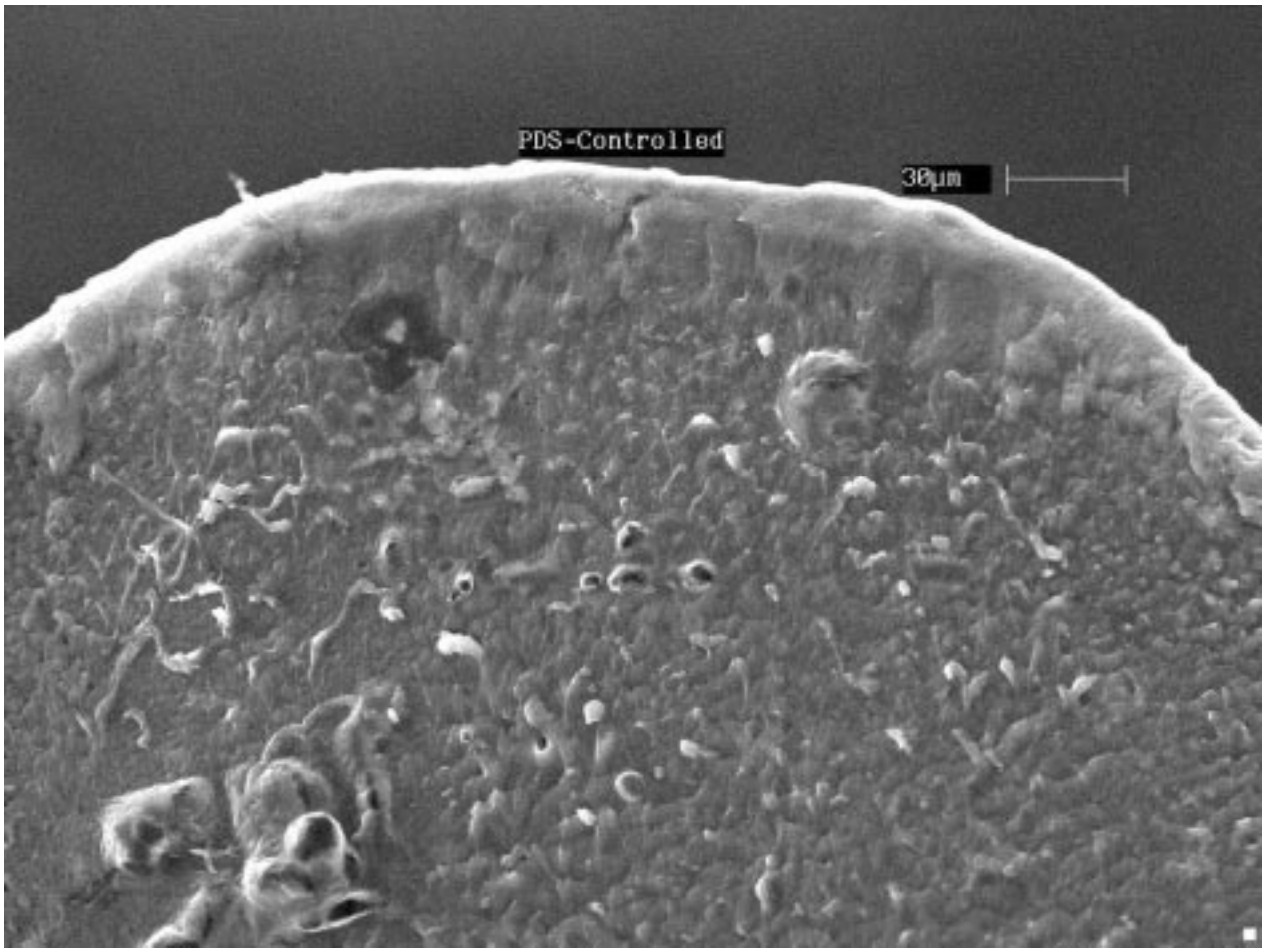

Figure 8 Scanning electron micrographs of the cross-sectional view of unhydrolyzed PDSII fiber to show its skin-core morphology.

LCM can reach. As illustrated in Fig. 2, only about 25% of the interior of the PDS II fiber (70 µm depth/130 µm radius) could be examined for pH change. This depth is limited both by the opacity of the sample and the working distance of the objective lens. A highly opaque material would not allow enough light intensity emitted from the fluorescent dye within the material back to the detector for proper imaging. Also, the fluorescent dye in the PDS-II fibers diffuses, diffracts and refracts the laser light from LCM, which means that the detector sees a lower intensity with increasing depth into the sample. Thus, the new technique should work the best with transparent biomaterials.

Another potential use of this technique is to analyze histological sections of biomaterials implanted *in vivo*. Such analysis would allow the measurement of pH in tissue adjacent to the implanted materials and possibly correlating the pH to any adverse tissue reactions. One challenge to developing such a method would be to ensure that the pH is preserved throughout the histological processing. Freeze-drying and cryosectioning would likely be useful for accomplishing this task.

Acknowledgments

This study was supported in parts by the research grants from the NIH (1-R03DE11199-01). We are grateful to Dr James Slattery of the Cornell University Biotechnology Program for his technical expertize and discussions about the LCM.

References

1. A. U. DANIELS, M. S. TAYLOR, K. P. ANDRIANO and J. HELLER, *Trans. 38th Ann. Mtg. Orthop. Res. Soc.* **17** (1992) 88.
2. M. S. TAYLOR, A. U. DANIELS, K. P. ANDRIANO and J. HELLER, *J. Appl. Biomater.* **5** (1994) 151–157.
3. J. EITENMÜLLER, K. L. GERLACH, T. SCHMICKAL, and G. MUHR, Die Versorgung von Sprunggelenksfrakturen unter Verwendung von Platten und Schrauben aus resorbierbarem Polymer material, presented at Jahrestagung der Deutschen Gesellschaft für Unfallheilkunde, Berlin, November 1989.
4. H. WINET and J. O. HOLLINGER, *J. Biomed. Mater. Res.* **27** (1993) 667.
5. O. BOSTMAN, E. HIRVENSALO *et al.*, *Intern. Orthop. (SICOT)* **14** (1990) 1.
6. G. O. HOFMANN, T. METZGER *et al.*, Biodegradable implants in traumatology – A review of the state of the art, XVIII SICOT Conference, Montreal, September 7, 1990, p. 190.
7. A. S. LITSKY, *J. Appl. Biomater.* **4** (1993) 109–111.
8. L. CLAES, in ''Clinical Implant Materials'', edited by G. HEIMKE, U. SOLTESZ and A. J. C. LEE, Elsevier, Amsterdam, pp. 161–167.
9. L. CLAES, in *''Biodegradable Implants in Orthopaedic Surgery''* edited by G. O. Hofmann, Kommunikation, Berlin, pp. 83–93.
10. K. E. REHM, H. J. HELLING *et al.*, in Jahrbuch der Chir, edited by H. Bunte, T. Junginger and A. Holzgreve edited by Biermann, Zulpich, 1989, pp. 223–32.
11. G. O. HOFMANN, *Clin. Mater.* **10** (1992) 75.
12. J. SUGANUMA, and H. ALEXANDER, *J. Appl. Biomater.* **4(1)** (1993) 13.
13. C. C. CHU, *Polymer* **26** (1985) 591–594.
14. M. HANTHAMRONGWIT, R. WILKINSON, C. OSBORNE,

W. H. REID, and M. H. GRANT, *J. Biomed. Mater. Res.* **30** (1996) 331–339.
15. M. A. SLIVKA, and C. C. CHU, *J. Biomed. Mater. Res.* **37(3)** (1997) 353–362.
16. M. VERT, S. M. LI, G. SPENLEHAUER and P. GUERIN, *J. Mater. Sci. Mater. Med.* **3** (1992) 423–446.
17. P. MAINIL-VARLET, R. CURTIS and S. GOGOLEWSKI, *J. Biomed. Mater. Res.* **36**(3) (1997) 360–380.
18. I. H. LOH, H. L. LIN and C. C. CHU, *J. Appl. Biomater.* **3**(2) (1992) 131–146.
19. E. BROYER, U. S. Patent 5,294,395, Ethicon, Inc., 1994.
20. C. C. CHU, J. A. VON FRAUNHOFER and H. P. GREISLER, ''Wound Closure Biomaterials and Devices'', (CRC Press, Boca Raton, FL, 1997) p. 147.
21. H. L. LIN, C. C. CHU and D. GRUBB, *J. Biomed. Mater. Res.* 27(2) (1993) 153.
22. L. E. SANZ, J. A. PATTERSON, R. KAMATH, G. WILLETT, S. W. AHMED and A. B. BUTTERFIELD, *Obstet. Gynecol.* **71** (1988) 418.
23. J. A. RAY, N. DODDI, D. REGULA, J. A. WILLIAMS, and A. MELVEGER, *Surg. Gynecol. Obstet.* **153** (1981) 497.
24. R. B. BOURNE, H. BITAR, P. R. ANDREAE, *et al.*, *Can. J. Surg.* **31** (1988) 43.
25. L. G. FRIBERG, G. W. MELLGREN, B. D. ERIKSSON, *et al.*, *Scand. J. Thorac. Cardiovasc. Surg.* **21** (1987) 9.
26. S. A. METZ, N. CHEGINI, and B. J. MASTERSON, *Biomaterials* **11** (1990) 41.

Received 4 December 1998
and accepted 19 November 1999